BBA - Biomembranes 1863 (2021) 183607

Contents lists available at ScienceDirect

BBA - Biomembranes

journal homepage: www.elsevier.com/locate/bbamem

Identification of a Dps contamination in Mitomycin-C–induced expression of Colicin Ia

Joka Pipercevic [a], Roman P. Jakob [a], Ricardo D. Righetto [b,1], Kenneth N. Goldie [b], Henning Stahlberg [b], Timm Maier [a], Sebastian Hiller [a,*]

[a] Biozentrum, University of Basel, 4056 Basel, Switzerland
[b] Center for Cellular Imaging and NanoAnalytics, Biozentrum, University of Basel, 4056 Basel, Switzerland

ARTICLE INFO

Keywords:
Colicin Ia
Protein purification
Mitomycin-C
SOS response
Protein contamination
Cryo-electron microscopy
2D crystallization

ABSTRACT

Colicins are bacterial toxins targeting Gram-negative bacteria, including *E. coli* and related *Enterobacteriaceae* strains. Some colicins form ion-gated pores in the inner membrane of attacked bacteria that are lethal to their target. Colicin Ia was the first pore-forming *E. coli* toxin, for which a high-resolution structure of the monomeric full-length protein was determined. It is so far also the only colicin, for which a low-resolution structure of its membrane-inserted pore was reported by negative-stain electron microscopy. Resolving this structure at the atomic level would allow an understanding of the mechanism of toxin pore formation. Here, we report an observation that we made during an attempt to determine the Colicin Ia pore structure at atomic resolution. Colicin Ia was natively expressed by mitomycin-C induction under a native SOS promotor and purified following published protocols. The visual appearance in the electron microscope of negatively stained preparations and the lattice parameters of 2D crystals obtained from the material were highly similar to those reported earlier resulting from the same purification protocol. However, a higher-resolution structural analysis revealed that the protein is Dps (DNA-binding protein from starved cells), a dodecameric *E. coli* protein. This finding suggests that the previously reported low-resolution structure of a "Colicin Ia oligomeric pore" actually shows Dps.

1. Introduction

Colicin Ia is a membrane pore-forming toxin in *E. coli*. It exerts its toxicity as a membrane-inserted form, which conducts ions to destroy a target membrane potential [1]. In the non-inserted form, colicin Ia is an α-helical protein of elongated Y-like shape [2]. The central R-domain is recognizing and binding to the outer membrane protein Cir [3,4] and is separated by a 160 Å coiled-coiled region from the lethal C-terminal channel-forming domain and the N-terminal T-domain [2]. The latter contains a TonB box [5], typical for TonB/Exb-dependent translocation along the outer membrane into the periplasmic space [6]. Its C-terminal channel-forming domain is made of ten α-helices [2] and is structurally similar to pore-forming domain of colicins E1, N and A [7–10], as well as to the T domain of diphtheria toxin [11] and Bcl-X_L [12]. The two central hydrophobic α-helices form a helical hairpin and are surrounded by amphipathic helices [13]. For Colicin Ia, it was shown that this helical hairpin can integrate into a lipid-bilayer in a voltage-independent manner [14]. The region containing amphipathic helices II–V (residues 474–541) are translocated through the lipid bilayer by an applied voltage [15,16]. From these single-channel conductance studies, it has been proposed that the helical hairpin together with a part of helix I and a region ranging from helices VI to VII are forming a four-transmembrane ion channel [16]. Two other studies based on the same method suggested that this channel has an hourglass shape [17,18] with a pore diameter of 1.8 nm at the cis-side, a diameter of 1 nm at the trans-side, and a restriction to around 7 Å in between the two entrances [17]. In stark contrast to these dimensions, Greig et al. presented a structure of the membrane-inserted Colicin Ia oligomer at a resolution of ~17 Å reconstituted in 2D crystals [19]. The structure featured a crown shape, with an outer diameter of 8.1 nm, an inner diameter of 3.4 nm and an averaged height of 4.3 nm.

Virtually all studies on colicin Ia reported so far, as well as studies on other colicins including Colicin K [20], Colicin E1 [21,22], Colicin E3 [23], used mitomycin-C (MMC) to stimulate the colicin overexpression.

* Corresponding author.
E-mail address: sebastian.hiller@unibas.ch (S. Hiller).
[1] Present address: Helmholtz Pioneer Campus, Helmholtz Zentrum München, Ingolstädter Landstraße 1, 85764 Neuherberg, Germany.

https://doi.org/10.1016/j.bbamem.2021.183607
Received 5 December 2020; Received in revised form 14 March 2021; Accepted 16 March 2021
Available online 26 March 2021

MMC is a natural antibiotic of *Streptomyces* and is a genotoxicant causing DNA damage [24]. DNA damage is repaired by SOS-response proteins [25] that are known to participate in different types of DNA repair mechanisms as well as in the eventual cell division arrest [26–29]. These proteins have characteristic LexA sites in their regulon that are also found in the regulon region of colicins [30]. Normally, a LexA dimer [31] represses the DNA transcription of SOS-response proteins. However, under conditions like DNA damage, an activator RecA enables their transcription while mediating [32] autocatalytical cleaving of repressor LexA [33]. MMC was found to cause DNA damage by DNA alkylation that can lead to a formation of DNA crosslinks [24]. In particular, DNA inter-crosslinks led to a strong SOS response in *E. coli*. Here, a single unrepaired DNA inter-crosslink can lead to a death of bacterium [24]. The alkylation of DNA occurred when MMC was in its reduced highly DNA-electrophilic mitosene form [34]. MMC alkylates the DNA preferably at 5′-CpG-3′ and 5′-GpG-3′ [35,36] positions; specifically on a 2-amino position of deoxyguanines located in a minor groove [37]. This enables introduction of an inter-strand [24] crosslink of 5′-CpG-3′ that reacts with the complementary deoxyguanine in 3′-GpC-5′ [37]. As well, an intra-strand crosslink [38] by a covalent bond between neighboring deoxyguanines in 5′-GpG-3′ are possible.

MMC was also shown to act as an oxidizing reagent. MMC gets reduced in presence of an oxygen and generates hydrogen peroxide [39]. Upon MMC treatment of *E. coli* cells in their exponential phase, expectedly, proteins that protect the cell from the oxidative stress like two catalases KatE and KatG [40] as well as DNA-binding protein from starved cells (Dps) [41,42] were found up-regulated on the transcriptional level [43]. Dps plays a protective role in starvation [41], extreme pH changes as well as upon exposure to heat, UV radiation and heavy metals [44]. Normally, Dps would only be present in minimal amounts during the bacterial exponential growth phase. This is different in the transition to stationary phase and especially during the stationary phase itself. In later phase, Dps is prominently expressed in a RhoS regulon-dependent way, reaching up to 20,000 molecules [41].

Structurally, electron-microscopy-based 2D projections of Dps revealed a ring-like shape with a diameter between 8 and 9 nm [41,45,46]. Dps is known to form hexagonal 2D crystals either in presence or absence of a non-specific DNA [41,46], respectively, assigning Dps a DNA protective role by biocrystalization [46]. Published X-ray structures reveal a hollow spherical dodecamer with a tetrahedral symmetry. The sphere has an inner diameter of 4.5 nm [47]. Its monomer has a four-helix bundle fold similar to structurally related bacterial ferritin [47]. The shell inside is highly negatively charged [47] and can harbor up to ~500 of iron(III) molecules [48].

Here, we report the result of a structural study aimed at elucidating the structure of the colicin Ia pore at atomic resolution. Colicin Ia was expressed by MMC treatment and purified. Structural studies that include negative-stain and cryo-electron microscopy of 2D crystals and X-ray crystallography suggest that the spherical particles observed previously arise from the contaminant Dps.

2. Materials and methods

2.1. Protein expression and purification

E. coli TG1 cells (Lucigen) were transformed with bacterial plasmid pKSJ340 obtained from Addgene (#27125), containing genes for Colicin Ia and the Colicin Ia immunity protein [49]. Cells were grown in LB medium at 37 °C to an OD_{600nm} of 0.7, whereupon Colicin Ia was induced by 0.5 μg/mL mitomycin-C (Roche). After 4 h, the culture was harvested at 7800 ×*g* by F9-6 × 1000 LEX fixed-angle rotor (Fiberlite, Thermofisher Scientific) and the cell pellet was resuspended in 50 mM boric acid/NaOH at pH 8.9 and 2 mM EDTA with additional protease inhibitors (Roche) and lysozyme, 5 mM $MgCl_2$ and DNAse I (Applichem). The cells were disrupted by sonication and centrifuged at 24,800 ×*g* by F14-14 × 50cy fixed-angle rotor (Fiberlite, Thermofisher Scientific) at 4 °C for 40 min. The cell lysate was applied on a 15 mL column, containing sulpho-propyl (SP) FF sepharose (GE Healthcare) of an Äkta purifier (GE Healthcare) system. The column was equilibrated with 50 mM boric acid/NaOH at pH 8.9 and 2 mM EDTA. The run was conducted by a flow rate of 0.5 mL/min. The column was washed with the respective buffer for 3 column volumes (CV) and subsequently the protein was elted by a 0–80% 1 M NaCl linear gradient. The fractions resulting from the cation ion exchange (CIEX) chromatography step and containing Colicin Ia were concentrated to 4.5 mL and applied on a Superdex 200 16/600 GL size-exclusion chromatography (SEC) column (GE Healthcare), which had been equilibrated with 20 mM sodium citrate at pH 5.2 and 50 mM NaCl. The volume of this column comprised 121 mL with a void volume around 48 mL. The flow rate used was 0.5 mL/min. A second size-exclusion chromatography step was included. The protein-containing fractions B5-B13 from first SEC step were pooled, concentrated to 0.4 mL and applied on a second Superdex 200 10/300 GL SEC column (GE Healthcare) with a column volume of 24 mL and a void volume around 8 mL. The running buffer was composed of 20 mM sodium citrate at pH 5.2 and 50 mM NaCl. The elution fraction was immediately flash frozen, stored at −80 °C and used for further experiments.

For 3D crystallization, Colicin Ia was labelled by selenomethionine. Hereby, the protein was expressed in one litre M9 culture with 4 g glucose as described in the section above with a slight difference. At an OD_{600nm} of 0.2–0.3 an amino acid mixture containing 100 mg lysine, 100 mg phenylalanine, 100 mg threonine, 50 mg isoleucine, 50 mg leucine, 50 mg valine and 100 mg DL-selenomethionine was added.

2.2. Reconstitution of Colicin Ia into lipids and 2D crystallization trials

1,2-Dimyristoyl-sn-glycero-3-phosphoglycerol (DMPG) and 1,2-Dimyristoyl-sn-glycero-3-phosphorylcholine (DPMC) were mixed in a ratio of 3:7 (*w*/w) and a supplement of 2% octyl-β glucoside in a buffer containing 20 mM sodium citrate at pH 5.2 and 50 mM NaCl. For a lipid-to-protein ratio (LPR, w/w) of 0.55 in a total volume of 2.2 mL, 0.9 mg/mL colicin Ia was added and incubated for 2 h at 37 °C. The sample was transferred to a 10 kDa MWCO dialysis cassette (Slide-A-Lyzer, Thermofisher Scientific) and dialysed against a buffer without detergent containing 50 mM sodium acetate at pH 4.5 and 150 mM NaCl for few days at 37 °C. After the dialysis, the sample was centrifuged at 21,100 ×*g* by FA-45-24-11 (Eppendorf) for 10 min. The soluble fraction and the pellet were both used for further studies. The soluble fraction was concentrated by *Vivaspin* (Sartorius) with 30 kDa MWCO. It was subsequently dialysed against 20 mM HEPES, pH 8.0 and 150 mM NaCl by exchanging buffer for several times by *Vivaspin* (Sartorius) with 30 kDa MWCO.

2.3. Negative-stain electron microscopy

For the preparation of negative-stain electron microscopy grids, 3.5 μL of protein sample was applied onto glow-discharged carbon grids and incubated for 1 min. The grids were blotted with filter paper and washed three times with MiliQ-water with blotting steps in-between. Staining was performed twice with 5 μL of 2% uranyl-acetate drops applied onto the grids with an incubation time of 0 and 30 s. Finally, the grids were blotted and air-dried for a minimum of 5 min. Micrographs were taken with a CM10 (Philips) transmission electron microscope (TEM), operated at 80 kV under 92,000× or 130,000× nominal magnification (pixel sizes 5.44 Å resp. 3.85 Å) and recorded with a Veleta CCD camera (EMSIS GmbH, Münster, Germany), or with a T12 (FEI) TEM, operated at 120 kV and recorded with a TVIPS F416 CMOS camera at a nominal magnification of 34,000× (pixel size 1.98 Å). The distances in recorded images were measured with the ImageJ 1.x software [50]. The particles resulting from the soluble fraction obtained after reconstitution of Colicin Ia into lipids were evaluated with the EMAN2 software [51]. For 2D classification, approximately 350 single particle images were picked

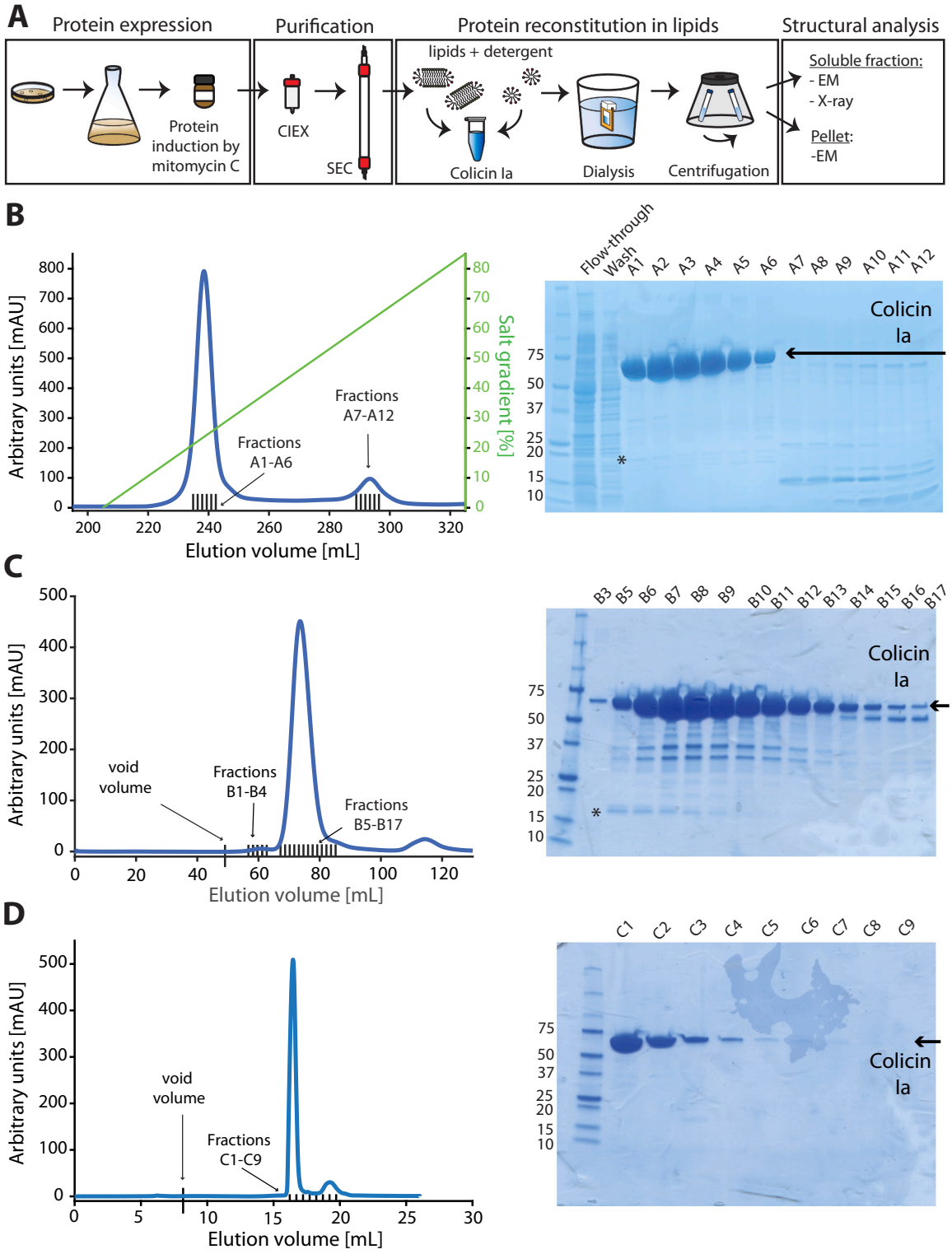

Fig. 1. Expression and purification of Colicin Ia. (A) A schematic overview of the Colicin Ia purification steps, its reconstitution into lipids and further structural studies. (B) Elution profile from cation exchange (CIEX) chromatography and its analysis by SDS-PAGE. Left lane - standard protein ladder, lane 2 – flow-through fraction, lane 3 – wash fraction, lanes 4–15 fractions of cation ion exchange run. (C) First size-exclusion chromatogram (SEC, with a Superdex 200 16/600 GL) and SDS-PAGE of collected fractions. Left lane - standard protein ladder, lane 2–15 are the fractions of respective size-exclusion chromatography. (D) Second size-exclusion chromatogram (SEC, with a Superdex 200 10/300 GL) and SDS-PAGE of size-exclusion chromatography fractions that are depicted on the left side. Lane 1 – standard protein ladder, lanes 2–15 are fractions of the size exclusion chromatography indicated in the left chromatogramm besides. Blue line – protein absorbance at 280 nm and green trendline depicted in (A) – 0–100% NaCl gradient. Arrows indicate collected fractions, void volume and proteins collected. Asterisks indicate the protein band of Dps.

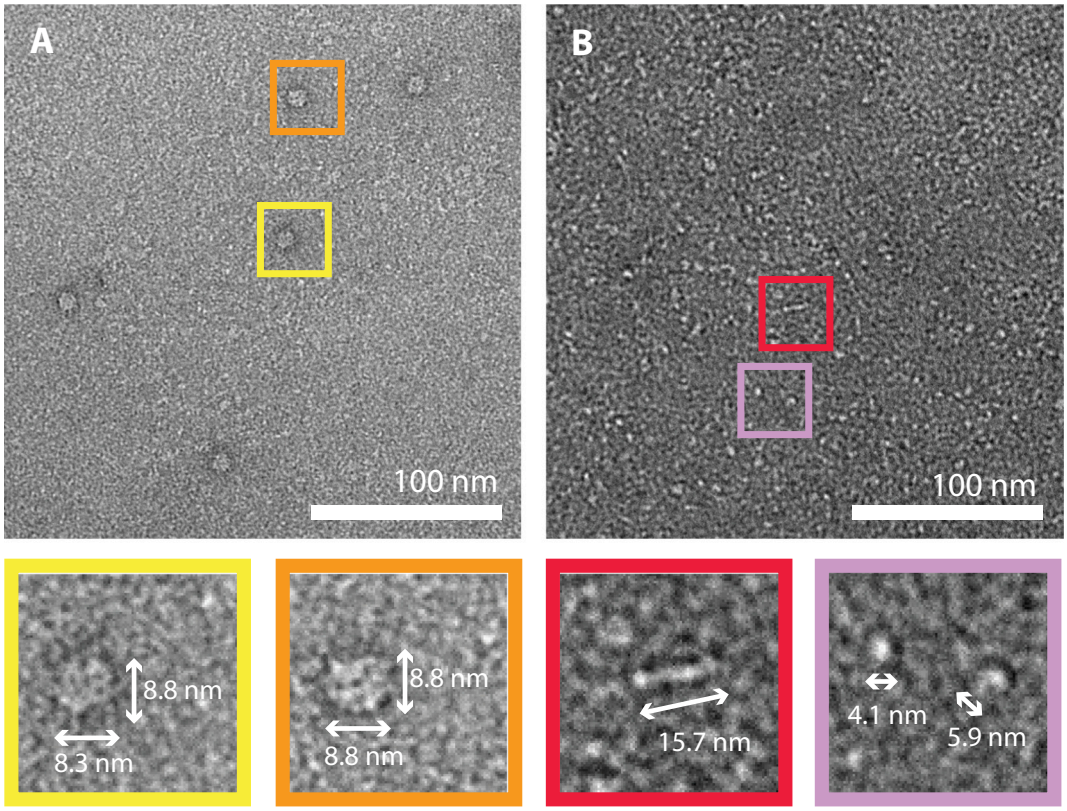

Fig. 2. Negative-stain electron microscopy of selected size-exclusion chromatography fractions. (A) Analysis of the concentrated fractions B1-B4 from first size-exclusion chromatography (see Fig. 1B). (B) Analysis of the fraction C1 from second size-exclusion chromatography (see Fig. 1C). Some of the particles indicated by a colored square in (A) and (B) were further magnified and are showed below in square of a corresponding color.

manually, CTF corrected and classified in 6 iterations into 24 classes with EMAN2.

2.4. Cryo-electron microscopy

3.5 μL of the soluble fraction after 2D crystallization trial and centrifugation was applied to 300-mesh lacey EM grid that had been covered with a 5 nm-thin carbon film and glow-discharged for 15 s. The protein sample was incubated on the grid for 1 min and blotted for 2 s on filter paper. Another 3.5 μL of the soluble fraction was again applied on the grid surface, incubated and blotted in the same way twice more. The grid was plunge frozen in liquid ethane using a FEI Vitrobot MK4 (Vitrobot, Maastrich Instruments) with 100% humidity in the chamber and a blotting time of 3 s. Micrographs were acquired with a T12 (FEI) operated at 120 kV and a TVIPS F416 camera at a nominal magnification of 54,000× and evaluated by 2dx [52] routines within the FOCUS [53] software.

2.5. 3D crystallization, data collection and structure determination of Dps

10.6 mg/mL Colicin Ia sample stored in 15 mM sodium acetate pH 4.5 and 150 mM NaCl was incubated with 0.5% octyl-β glucoside at 37 °C for 45 min. 3D crystals were obtained by a sitting-drop vapor diffusion experiments in a 2:1 ratio of protein and precipitant at room temperature. They grew to their final size within one week. Crystals were cryo-preserved by addition of ethylene glycol to a final concentration of 20% (*v*/v) and flash cooled in liquid nitrogen. Six data sets of a single crystal were collected at the SLS beamline X06DA (Swiss Light Source, Paul Scherrer Institute, Switzerland) at 100 K and were integrated, indexed and scaled using XDS software [54,55]. The crystal structure was determined by SeMet-SAD phasing and refined at 2.80 Å. Selenium sites were identified in the Se-Met dataset by Phenix-HySS [56]. Initial automated model building was carried out with Phenix [57] and Buccaneer [58] and suggested a dodecameric structure with homology to ferritin. Following molecular replacement using PDB ID: 1DPS [47] revealed unambiguously, that the crystal consists of Dps dodecamers only. Based on this replacement solution, manual model building and structure refinement were performed with Coot [59] and PHENIX [60]. Model quality was validated with Molprobity [61]. Data collection and refinement statistics are summarized in Table S2. The atomic coordinates and structure factors have been deposited in the Protein Data Bank under PDB ID: 7AQS.

2.6. Liposome pull-down assay

Liposomes were prepared from one of the following lipids: *E. coli* polar extract (*Avanti*), Soybean polar extract (*Avanti*), DMPC:DMPG (*Avanti*) in a 3:7 (*w*/w) ratio. The respective lipids were dried with argon gas and left in an exicator overnight at room temperature. The lipid biofilm was dissolved in 20 mM Tris pH 7.5 and 100 mM NaCl to a lipid concentration of 10 mg/mL and were incubated for 3 h at a room temperature. Several cycles of freezing in liquid nitrogen and thawing at 42 °C were performed. Lipid samples were applied 10 times on a pressure-based extruder through a polycarbonate membrane of 100 nm. Dynamic light scattering on a Zetasizer Nano ZS (*Malvern Panalytical*) was used to verify the homogeneity of liposomes. Lipids were incubated with 0.9 mg/mL protein at different pH by using one of the following buffers and in 150 mM NaCl; 75 mM Sodium acetate pH 4.5, 50 mM MES pH 6.5 or 50 mM Tris pH 8.0. An analytical ultracentrifugation was conducted on an Optima MAX XP (*Beckman*) with a TLA 120.1 rotor at 100,000 rpm for 1 h.

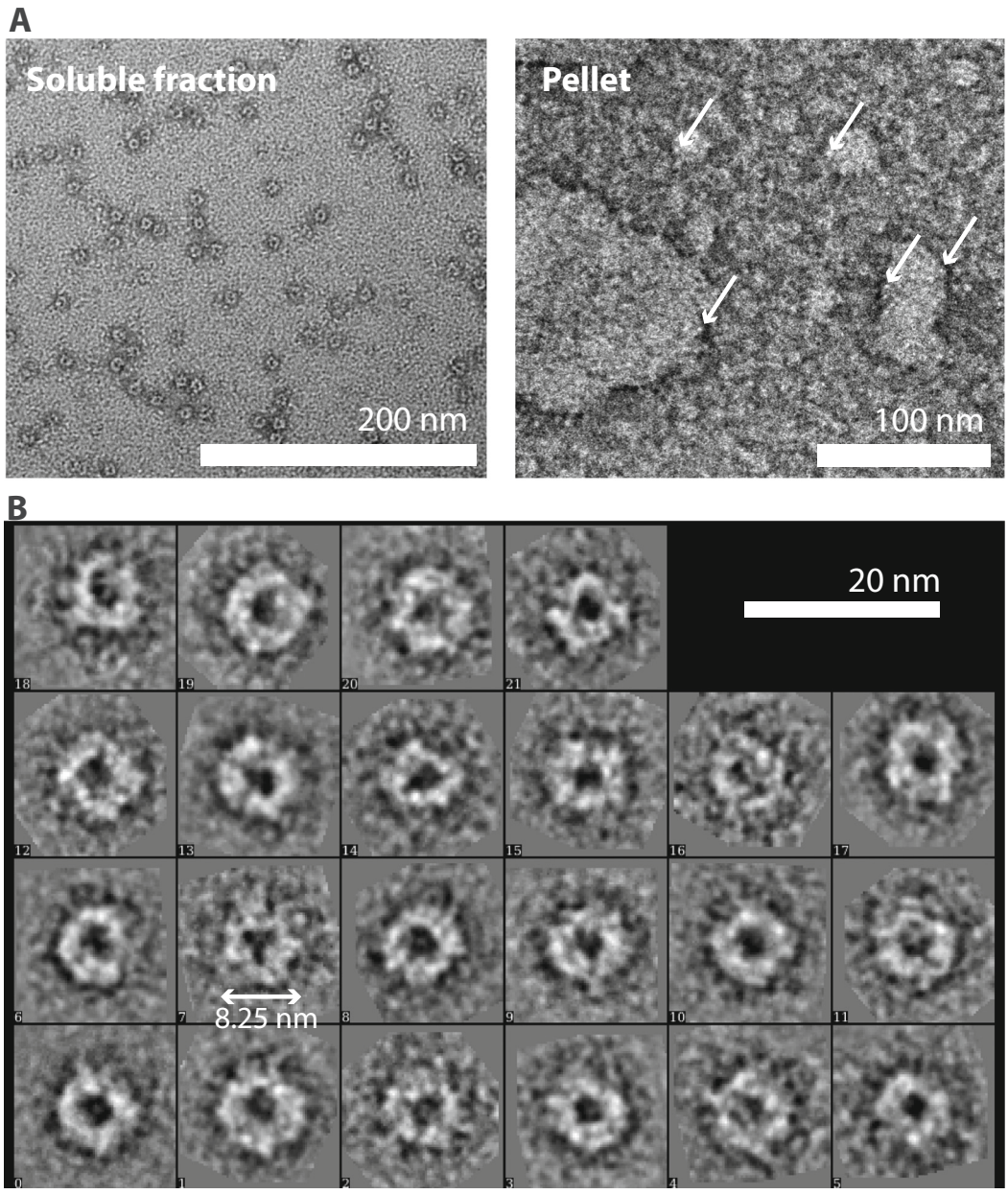

Fig. 3. Analysis of soluble fraction and pellet after Colicin Ia is reconstituted into lipids. (A) Protein sample containing Colicin Ia (elution fraction C1-C3 from 1D) was incubated with detergent and lipids and subsequently dialysed in a buffer at pH 4.5 without detergent. After the centrifugation step, both, the soluble fraction, left side, and the pellet, right side, obtained were analysed by negative-stain electron miscroscopy. Arrows indicate protein within the lipidic membranes. (B) 2D classification of particles from the soluble fraction.

2.7. LC-MS/MS analysis

Protein samples were dissolved in digestion buffer (100 mM Tris-HCl, pH 8.0, 6 M urea, 10 mM DTT) and reduced at 37 °C for 1 h. After adding iodoacetamide to a final concentration of 20 mM, reduced disulfide bonds were alkylated at 25 °C for 30 min in the dark. Subsequently, urea was diluted to 1.5 M by adding 30 μL 100 mM Tris-HCl, pH 8.0, and the sample was digested with endoproteinase LysC (1/100, *w*/w; Wako) for 2 h at 37 °C. The digest was diluted by adding 60 μL 100 mM Tris-HCl, pH 8.0 and digestion was continued with trypsin (1/50, w/w; Promega) for 18 h at 37 °C. The digest was acidified with trifluoroacetic acid to a 1% final concentration and the sample was desalted on a MicroSpin cartridge (The Nest Group). The peptides were dried and analysed by capillary LC-MS/MS using a 300SB C-18 trap column (0.3 × 50 mm) (Agilent Technologies) connected to a 0.1 mm × 10 cm capillary separation column packed with Magic C18 (5 μm particle diameter). The capillary column was connected to an Orbitrap FT hybrid instrument (Thermo Finnigan). A linear gradient from 2 to 60% solvent B (0.1% acetic acid and 80% acetonitrile in water) in solvent A (0.1% acetic acid and 2% acetonitrile in water) in 85 min was delivered with an Agilent 1260 nano pump at a flow of 0.5 μL min^{-1}. A 10 μL volume of sample was injected with an autosampler set to 4 °C onto the trap column. The eluting peptides were ionized at 1.6 kV. The mass spectrometer was operated in a data-dependent fashion so that peptide ions were automatically selected for fragmentation by collision-induced dissociation (MS/MS) in the Orbitrap. The MS/MS spectra were searched against a *E. coli* protein database using Proteome Discoverer 1.4 (Thermo Scientific) using the two search engines Mascot and SequestHT. For the search, oxidized methionine, N-terminal protein acetylation were used as variable modifications, carbamidomethylation

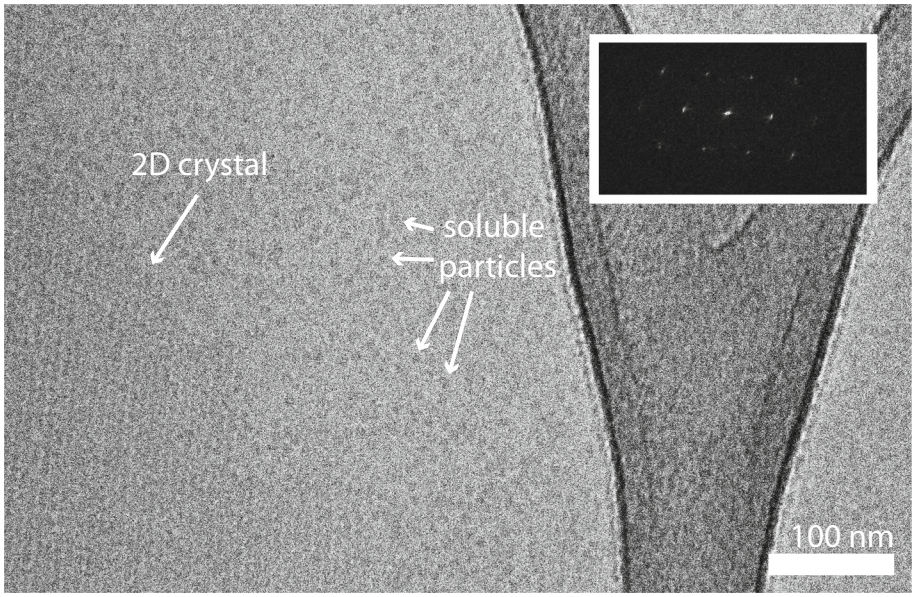

Fig. 4. Soluble fraction obtained after Colicin Ia is reconstituted into lipids can form 2D crystals. Cryo-electron microscopy of the soluble fraction obtained after reconstitution of Colicin Ia in lipids. 2D crystals were formed upon a pH shift from pH 4.5 to pH 8. White arrows indicate 2D crystal and soluble particles. Upper right corner displays Fourier transformation of masked 2D crystal.

of cysteines was set as a fixed modification. The identifications were filtered to a false discovery rate of 1%.

3. Results

3.1. Ring-like shaped particles observed during purification of Colicin Ia

Colicin Ia was expressed and purified following a published protocol [19]. In brief, colicin Ia was induced by MMC at an OD_{600nm} of 0.7, and expression continued for 4 h (Fig. 1A) [19]. DNA was removed by DNAse I and Colicin Ia was purified by cation ion-exchange chromatography and subsequent size-exclusion chromatography (Fig. 1A). Already the first purification step by cation-exchange chromatography yielded highly pure Colicin Ia (Fig. 1B). In the second purification step by size exclusion chromatography, three elution peaks were observed (Fig. 1C). The fractions collected from peaks at 60 mL and 75 mL indicated the presence of a protein with a size between 50 and 75 kDa, as revealed by SDS-PAGE. This is in accordance with the size of monomeric Colicin Ia of 69 kDa. The identity of the protein was further confirmed by mass spectrometry. As Colicin Ia was observed to degrade over time, the Colicin Ia fractions were subjected to a second round of size-exclusion chromatography, yielding pure Colicin Ia with no significant impurities visible in SDS-PAGE (fraction C1 in Fig. 1D). Negative-stain electron microscopy after the first SEC revealed soluble particles of spherical shape with approx. 8.5 nm diameter (Fig. 2A). TEM images after the second SEC showed smaller particles below 6 nm diameter, and less frequently some elongated shapes of up to 15.7 nm length (Fig. 2B). The smaller spherical particles likely correspond to end-on views of Colicin Ia, while the elongated shape corresponded well to the published X-ray structure of soluble monomeric Colicin Ia [2], with a coiled-coiled region of around 160 Å separating the receptor binding R-domain from the membrane channel-forming C-domain and the N- terminal T-domain.

As mentioned above, the first size-exclusion chromatography displayed peaks at 60 mL, 75 mL and 115 mL. The first elution peak of 61 mL corresponded to an effective protein size between 158 and 440 kDa. Negative-stain electron micrographs of this sample displayed ring-shaped soluble particles of a diameter between 8 nm and 9 nm (Fig. 2A). These particles are visually highly similar to previously reported Colicin Ia oligomers that were obtained upon incubating Colicin Ia with detergents and lipids and subsequent dialysis [19]. At the same time, these 2D projections also resemble the Dps oligomer [41,45,46], an endogenous *E. coli* protein of around 19 kDa that can form a dodecamer of around 220 kDa in size [47]. The presence of Dps monomers was further evident as faint protein bands in the fractions obtained by cation ion-exchange chromatography (asterik in the Fig. 1B) and size-exclusion chromatography (asterik in the Fig. 1C). The identity of Dps was additionally confirmed by liquid chromatography coupled to mass-spectrometry (LC-MS/MS) of the elution peak (Supplementary Table 1).

Table 1
Comparison of ring-shaped particles obtained in different studies.

	Colicin Ia	Dps	This study
Soluble particles in EM	Ring-like ~8 nm [19]	Ring-like ~9 nm [41,45,46]	Ring-like 8–9 nm
Unit cell lattice of 2D crystal	Hexagonal packing: a = b = 94 Å, γ = 120° [19]	Hexagonal packing: a = b = 78 Å, γ = 120° [46]	Hexagonal packing: a = 90 Å, b = 92 Å, γ = 120°

3.2. Reconstitution into lipids yields 2D crystals of ring-like shaped particles

A reconstitution of soluble Colicin Ia in a lipid bilayer was performed following published protocols [19]. Briefly, lipids DMPC and DMPG were mixed in a ratio of 3:7 (*w*/w) and supplemented by 2% of octyl-ß glucoside (Fig. 1A). Colicin Ia and lipids were incubated in a lipid-to-protein ratio of 0.55. This sample was dialyzed extensively against a buffer with a pH of 4.5 and no detergent (Fig. 1A). After the dialysis, the soluble fraction and the pellet containing lipid-bound protein were obtained by a centrifugation step (Fig. 1A). They were further analysed by negative-stain electron microscopy.

The soluble fraction of the dialyzed sample contained ring-like shaped particles. They were visually similar to the particles obtained during size-exclusion chromatography (Fig. 3A). The 2D classification of particles from the soluble fraction showed for all classes ring-shaped particles with an approximate diameter of 8 nm (Fig. 3B). This suggests that the protein either had a preferential orientation on the electron

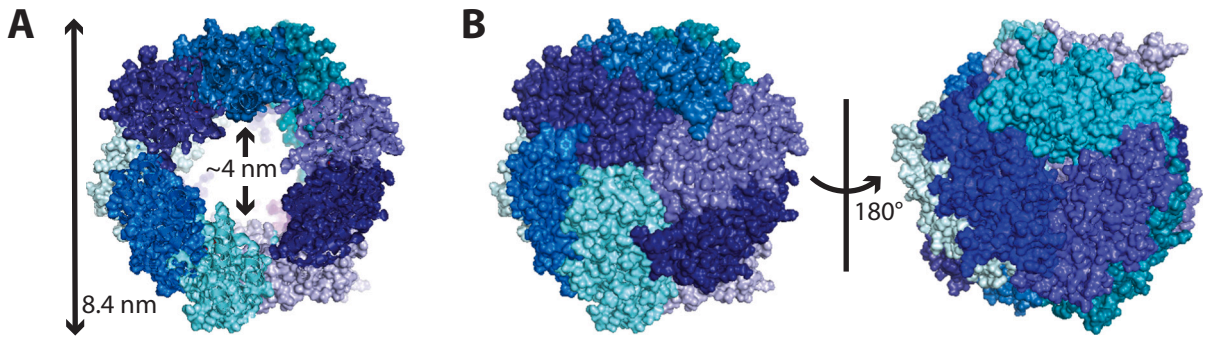

Fig. 5. Atomic resolution structure of Dps. (A) Cross-section through the Dps dodecamer. Different colors represent single Dps monomers. The arrows indicate the size of the outer and the inner diameter of the Dps oligomer. (B) Side view on the complete Dps dodecamer. The protein forms a hollow sphere.

microscopy grids or that the protein is formed as a hollow sphere, so that all projections resemble a ring. A further treatment of the soluble fraction by changing the pH from 4.5 to a pH of 8 led to the formation of 2D crystals (Fig. 4). These were found to have a hexagonal packing and cell unit parameters a = 90 Å, b = 92 Å and γ = 120° (Table 1). These values are very similar to reported 2D crystal parameters of a proposed Colicin Ia oligomer (Table 1) [19].

A preliminary analysis by negative stain electron microscopy was also performed on the re-suspended pellet obtained after reconstitution of Colicin Ia in lipids. This revealed the presence of membrane patches of irregular texture, compatible with the presence of reconstituted but not crystalline membrane proteins in the lipid bilayers (Fig. 3B). Furthermore, a lipid-pull down assay confirmed that Colicin Ia at pH 4.5 is exclusively associated with the lipid fraction in the pellet (Supplementary Fig. 1). However, in our hands we did not notice the formation of well-ordered 2D crystals at pH 4.5 as reported earlier [19].

3.3. Formation of 3D crystals from the Colicin Ia sample

The Colicin Ia sample was utilized in two different ways for X-ray crystallization experiments. Firstly, the soluble fraction obtained after reconstitution of Colicin Ia in lipids was used for setting-up the crystallization plates (Fig. 1A). It contained ring-like shaped particles (Fig. 3A) similar to those published earlier [19] that were suggested to represent an oligomeric pore of Colicin Ia. Secondly, the protein sample was incubated with a detergent - octyl-β glucoside or n-dodecyl β-D-maltoside (DDM), respectively. The rationale behind this was that electrophysiological studies of Colicin Ia had reported that detergents can lead to an increased amount of Colicin Ia channels formed in a lipidic bilayer if compared to non-treated Colicin Ia [14]. This was suggesting that some detergents can shift the conformational equilibrium between soluble and oligomeric Colicin Ia, which could possibly lead to crystals of oligomeric Colicin Ia. Protein 3D crystals were obtained from both sample preparations. The structure of the crystals was determined by selenomethionine-labeling. The structure obtained is a dodecameric sphere with a tetrahedral symmetry, identical to the known structure of Dps (PDB ID: 1DPS) [47] (Fig. 5, Table 1 and Supplementary Table 2).

4. Discussion

When aiming at a high-resolution structure of the membrane-inserted Colicin Ia oligomer, we purified and reconstituted protein particles that were resembling and reported oligomeric Colicin Ia [19] in size and visual appearance, but at the same time also the protein Dps [41,45,46] (Table 1). 2D crystallization attempts resulted in a pellet fraction that upon preliminary TEM inspection showed membrane patches of irregular structure but did not show well-ordered 2D crystals. In view of the recent improvements of single particle cryo-EM, 2D crystallization attempts were not pursued further. However, well-ordered 2D crystals were obtained from particles from the soluble fraction that showed in projection images a ring-like appearance. Such particles were observed as a minor population after the first purification step, and such particles were also observed in the soluble fraction after membrane reconstitution attempts. A pH change from 4.5 to 8 for the soluble fraction then produced well-ordered 2D crystals that had very similar lattice parameters as those reported from an alleged reconstruction of the oligomeric Colicin pore [19]. However, Dps is also known to form 2D crystals with similar hexagonal packing [41,46] (see Table 1).

It appears highly unlikely that the particles obtained in the soluble fraction after reconstitution of Colicin Ia into lipids were membrane-bound Colicin Ia. In lipid-pull down experiments under the same conditions, soluble Colicin Ia shifted completely to the lipid-bound state, indicating that it is not soluble at these conditions. Hence, the particles obtained in the soluble fraction were most likely a contaminating other protein. In our 3D crystallization experiments, the protein Dps was successfully crystalized from the Colicin Ia sample, (Table 1) indicating that Dps was present as a co-purified product. The high amounts of Dps were most likely due to the induction of Colicin Ia expression by MMC, which is known to also significantly increase the amount of Dps in *E. coli* [43]. Additionally, the purification protocol employed contained a cation ion-exchange step that favors Dps binding as well. Dps is known to get extracted natively without tags, while bound to hydroxyl-group rich agarose-based sepharose 6B and eluting with 200 mM NaCl [41]. In this study, the ion-exchange material used was agarose-based sulphopropyl (SP) sepharose that has similar properties.

Taken together, our results thus suggest that the previously reported low-resolution structure of oligomeric Colicin [19] was a misinterpretation and actually represented the contaminant Dps. Our protein expression and purification protocol of Colicin Ia followed the earlier report [19], making it likely that the earlier study also co-purified Dps. Because the publication of Greig et al. [19] is as of today the only report describing colicin as forming a large pore in its membrane-inserted form, we suggest that the membrane-inserted form of Colicin Ia is likely smaller [16,17].

Declaration of competing interest

The authors declare that they have no known competing financial interests or personal relationships that could have appeared to influence the work reported in this paper.

Acknowledgments

We thank Mohamed Chami for help with 2D crystallization. J.P was supported by Fellowship for Excellence granted by Biozentrum belonging to University of Basel.

Appendix A. Supplementary data

Supplementary data to this article can be found online at https://doi.org/10.1016/j.bbamem.2021.183607.

References

[1] S.J. Schein, B.L. Kagan, A. Finkelstein, Colicin K acts by forming voltage-dependent channels in phospholipid bilayer membranes, Nature. 276 (1978) 159–163.
[2] M. Wiener, D. Freymann, P. Ghosh, R. Stroud, Crystal structure of colicin Ia, Nature. 385 (1997) 461–464.
[3] B.S. Cowell, J. Konisky, Interaction of Colicin Ia with bacterial cells. Direct measurement of Ia-receptor Interaction, J. Biol. Chem. 247 (1972) 6524–6529.
[4] S.K. Buchanan, P. Lukacik, S. Grizot, R. Ghirlando, M.M.U. Ali, T.J. Barnard, K. S. Jakes, P.K. Kienker, L. Esser, Structure of colicin I receptor bound to the R-domain of colicin Ia: implications for protein import, EMBO J. 26 (2007) 2594–2604, https://doi.org/10.1038/sj.emboj.7601693.
[5] E. Schramm, J. Mende, V. Braun, R.M. Kamp, Nucleotide sequence of the colicin B activity gene cba: consensus pentapeptide among TonB-dependent colicins and receptors, J. Bacteriol. 169 (1987) 3350–3357.
[6] V. Braun, Energy-coupled transport and signal transduction through the Gram-negative outer membrane via TonB-ExbB-ExbD-dependent receptor proteins, FEMS Microbiol. Rev. 16 (1995) 295–307.
[7] M.W. Parker, F. Pattus, A.D. Tucker, D. Tsernoglou, Structure of the membrane-pore-forming fragment of colicin A, Nature. 337 (1989) 93–96.
[8] P. Elkins, A. Bunker, W.A. Cramer, C.V. Stauffacher, A mechanism for toxin insertion into membranes is suggested by the crystal structure of the channel-forming domain of colicin E1, Structure 5 (1997) 443–458.
[9] I.R. Vetter, M.W. Parker, A.D. Tucker, J.H. Lakey, F. Pattus, D. Tsernoglou, Crystal structure of a colicin N fragment suggests a model for toxicity, Structure. 6 (1998) 863–874.
[10] S.D. Zakharov, E. e Kotova, Y.N. Antonenko, W. a Cramer, On the role of lipid in colicin pore formation, Biochim. Biophys. Acta 1666 (2004) 239–249, https://doi.org/10.1016/j.bbamem.2004.07.001.
[11] M.J. Bennett, D. Eisenberg, et al., Protein Sci. 3 (1994) 1464–1475.
[12] S.W. Muchmore, M. Sattler, H. Liang, R.P. Meadows, J.E. Harlan, H.S. Yoon, D. Nettesheim, B.S. Chang, C.B. Thompson, S.L. Wong, S.L. Ng, S.W. Fesik, X-ray and NMR structure of human Bcl-xL, an inhibitor of programmed cell death, Nature. 381 (1996) 335–341, https://doi.org/10.1038/381335a0.
[13] S.D. Zakharov, W.A. Cramer, Colicin crystal structures: pathways and mechanisms for colicin insertion into membranes, Biochim. Biophys. Acta 1565 (2002) 333–346.
[14] P.K. Kienker, X.-Q. Qiu, S.L. Slatin, A. Finkelstein, K.S. Jakes, Transmembrane insertion of the Colicin Ia hydrophobic hairpin, J. Membr. Biol. 157 (1997) 27–37.
[15] S.L. Slatin, X. Qiu, K.S. Jakes, A. Finkelstein, Identification of a translocated protein segment in a voltage-dependent channel, Nature. 371 (1994) 158–161.
[16] X. Qiu, K.S. Jakes, P.K. Kienker, A. Finkelstein, Major transmembrane movement associated with Colicin Ia channel gating, J. Gen. Physiol. 107 (1996) 313–328.
[17] O.V. Krasilnikov, J.B. Da Cruz, L.N. Yuldasheva, W.A. Varanda, R.A. Nogueira, A novel approach to study the geometry of the water lumen of ion channels: colicin Ia channels in planar lipid bilayers, J. Membr. Biol. 92 (1998) 83–92.
[18] P.K. Kienker, K.S. Jakes, A. Finkelstein, Identification of channel-lining amino acid residues in the hydrophobic segment of colicin Ia, J. Gen. Physiol. 132 (2008) 693–707, https://doi.org/10.1085/jgp.200810042.
[19] S.L. Greig, M. Radjainia, A.K. Mitra, Oligomeric structure of colicin ia channel in lipid bilayer membranes, J. Biol. Chem. 284 (2009) 16126–16134, https://doi.org/10.1074/jbc.M900292200.
[20] S.-S. Tsao, W.F. Goebel, K. Colicin, 8. The immunological properties of mitomycin-induced colicin K, J. Exp. Med. 130 (1969) 1313–1335.
[21] K.S. Jakes, C.K. Abrams, A. Finkelstein, S.L. Slatin, Alteration of the pa-dependent ion selectivity channel by site-directed mutagenesis of the Colicin, J. Biol. Chem. 265 (1990) 6984–6991.
[22] K.S. Jakes, The Colicin E1 TolC box: identification of a domain required for Colicin E1 cytotoxicity and TolC binding, J. Bacteriol. 199 (2017) e00412–e00416.
[23] K.S. Jakes, N.D. Zinder, Highly purified Colicin E3 contains immunity protein, PNAS. 71 (1974) 3380–3384.
[24] W. Szybalski, W.N. Iyer, Crosslinking of DNA by enzymatically or chemically activated mitomycins and porfiromycins, bifunctionally “alkylating” antibiotics, Fed. Proc. 23 (1964) 946–957. http://europepmc.org/abstract/MED/14209827.
[25] W.L. Kelley, Lex marks the spot: the virulent side of SOS and a closer look at the LexA regulon, Mol. Microbiol. 62 (2006) 1228–1238, https://doi.org/10.1111/j.1365-2958.2006.05444.x.
[26] M. Radman, SOS repair hypothesis: phenomenology of an inducible DNA repair which is accompanied by mutagenesis, in: P.C. Hanawalt, R.B. Setlow (Eds.), Mol. Mech. Repair DNA, Basic Life, Springer, Boston, MA, 1975, pp. 355–367, https://doi.org/10.1007/978-1-4684-2895-7_48.
[27] J.W. Little, D.W. Mount, The SOS regulatory Escherichia coli system, Cell. 29 (1982) 11–22.
[28] G.C. Walker, The SOS response of Escherichia coli, in: F. Neidhardt, J. Ingraham, K. Low, B. Magasanik, M. Schaechter, H. Umbarger (Eds.), *Escherichia coli* Salmonella Typhimurium, Cellular A, American Society for Microbiology, Washington, DC, US, 1987, pp. 1346–1357.
[29] E.C. Friedberg, G.C. Walker, W. Siede, R.D. Wood, R. Schultz, T. Ellenburger, DNA Repair and Mutagenesis, 2nd ed., American Society for Microbiology Press, Washington, DC, 2006.
[30] O. Gillor, J.A.C. Vriezen, M.A. Riley, The role of SOS boxes in enteric bacteriocin regulation, Microbiology 154 (2009) 1783–1792, https://doi.org/10.1099/mic.0.2007/016139-0.The.
[31] K.C. Giese, C.B. Michalowski, J.W. Little, RecA-dependent cleavage of LexA dimers, J. Mol. Biol. 377 (2009) 148–161.
[32] L.-L. Lin, J.W. Little, Autodigestion and RecA-dependent cleavage of Ind- mutant LexA proteins, J. Mol. Biol. 210 (1989) 439–452.
[33] J.W. Little, Autodigestion of lexA and phage lambda repressors, PNAS. 81 (1984) 1375–1379.
[34] G.S. Kumar, R. Lipman, J. Cummings, M. Tomasz, Mitomycin C - DNA adducts generated by DT-diaphorase. Revised mechanism of the enzymatic reductive activation of mitomycin C, Biochemistry 36 (1997) 14128–14136, https://doi.org/10.1021/bi971394i.
[35] V.-S. Li, H. Kohn, Studies on the bonding specificity for mitomycin C-DNA monoalkylation processes, JACS. 113 (1991) 275–283, https://doi.org/10.1021/ja00001a040.
[36] S. Kumar, R. Lipman, M. Tomasz, Recognition of specific DNA sequences by mitomycin C for alkylation, Biochemistry. 31 (1992) 1399–1407, https://doi.org/10.1021/bi00120a016.
[37] M. Tomasz, D. Lipman, Roselyn Chowdary, J. Pawlak, G.L. Verdine, K. Nakanishi, Isolation and structure of a covalent cross-link adduct between mitomycin C and DNA, Science 235 (1987) 1204–1208.
[38] R. Bizanek, B.F. McGuinness, K. Nakanishi, M. Tomasz, Isolation and structure of an intrastrand cross-link adduct of mitomycin C and DNA, Biochemistry. 31 (1992) 3084–3091, https://doi.org/10.1021/bi00127a008.
[39] M. Tomasz, H2O2 generation during the redox cycle of mitomycin C and dna-bound mitomycin C, Chem. Biol. Interact. 13 (1976) 89–97, https://doi.org/10.1016/0009-2797(76)90016-8.
[40] P.C. Loewen, J. Switala, B.L. Triggs-Raine, Catalases HPI and HPII in Escherichia coli are induced independently, Arch. Biochem. Biophys. 243 (1985) 144–149.
[41] M. Almiron, A.J. Link, D. Furlong, R. Kolter, A novel DNA-binding protein with regulatory and protective roles in starved Escherichia coli, Genes Dev. 6 (1992) 2646–2654.
[42] A. Martinez, R. Kolter, Protection of DNA during oxidative stress by the nonspecific DNA-binding protein Dps, J. Bacteriol. 179 (1997) 5188–5194.
[43] P.P. Khil, R.D. Camerini-otero, Over 1000 genes are involved in the DNA damage response of Escherichia coli, Mol. Microbiol. 44 (2002) 89–105.
[44] S. Nair, S.E. Finkel, Dps protects cells against multiple stresses during stationary phase, J. Bacteriol. 186 (2004) 4192–4198, https://doi.org/10.1128/JB.186.13.4192.
[45] Y. Zhang, J. Fu, S.Y. Chee, E.X.W. Ang, B.P. Orner, Rational disruption of the oligomerization of the mini-ferritin E. coli DPS through protein-protein interface mutation, Protein Sci. 20 (2011) 1907–1917, https://doi.org/10.1002/pro.731.
[46] S.G. Wolf, D. Frenkiel, T. Arad, S.E. Finkel, R. Kolter, A. Minsky, DNA protection by stress-induced biocrystallization, Nature. 400 (1999) 83–85.
[47] R.A. Grant, D.J. Filman, S.E. Finkel, R. Kolter, J.M. Hogle, The crystal structure of Dps, a ferritin homolog that binds and protects DNA, Nature. 5 (1998) 294–303.
[48] G. Zhao, P. Ceci, A. Ilari, L. Giangiacomo, T.M. Laue, E. Chiancone, N.D. Chasteen, N. Hampshire, C.S.B. Molecolare, S. Biochimiche, L. Sapienza, Iron and hydrogen peroxide detoxification properties of DNA-binding protein from starved cells. a ferritin-like DNA-binding protein of *Escherichia coli*, J. Biol. Chem. 277 (2002) 27689–27696, https://doi.org/10.1074/jbc.M202094200.
[49] K.S. Jakes, A. Finkelstein, The colicin Ia receptor, Cir, is also the translocator for colicin Ia, Mol. Microbiol. 75 (2010) 567–578, https://doi.org/10.1111/j.1365-2958.2009.06966.x.
[50] C.A. Schneider, W.S. Rasband, W.K. Eliceiri, NIH Image to ImageJ: 25 years of image analysis, Nat. Methods 9 (2012) 671–675.
[51] G. Tang, L. Peng, P.R. Baldwin, D.S. Mann, W. Jiang, I. Rees, S.J. Ludtke, EMAN2: an extensible image processing suite for electron microscopy, J. Struct. Biol. 157 (2007) 38–46.
[52] B. Gipson, X. Zeng, Z.Y. Zhang, H. Stahlberg, 2dx — user-friendly image processing for 2D crystals, J. Struct. Biol. 157 (2007) 64–72, https://doi.org/10.1016/j.jsb.2006.07.020.
[53] N. Biyani, R.D. Righetto, R. Mcleod, D. Caujolle-bert, D. Castano-diez, K.N. Goldie, H. Stahlberg, Focus: the interface between data collection and data processing in, J. Struct. Biol. 198 (2017) 124–133, https://doi.org/10.1016/j.jsb.2017.03.007.
[54] W. Kabsch, Integration, scaling, space-group assignment and post-refinement, Biol. Crystallogr. 66 (2010) 133–144, https://doi.org/10.1107/S0907444909047374.
[55] W. Kabsch, XDS, Biol. Crystallogr. 66 (2010) 125–132, https://doi.org/10.1107/S0907444909047337.
[56] P.H. Zwart, P.V. Afonine, L.W. Grosse-Kunstleve, R.W. Hung, T.R. Ioerger, A. J. McCoy, E. McKee, N.W. Moriarty, R.J. Read, J.C. Sacchettini, N.K. Sauter, L. C. Storoni, T.C. Terwilliger, P.D. Adams, Automated structure solution with the PHENIX suite, Methods Mol. Biol. 426 (2008) 419–435.
[57] T.C. Terwilliger, P.V. Grosse-Kunstleve, Ralf W. Afonine, N.W. Moriarty, P. H. Zwart, L.-W. Hung, R.J. Read, P.D. Adams, Iterative model building, structure refinement and density modification with the PHENIX AutoBuild wizard, Biol. Crystallogr. 64 (2008) 61–69, https://doi.org/10.1107/S090744490705024X.
[58] K. Cowtan, The Buccaneer software for automated model building. 1. Tracing protein chains, Biol. Crystallogr. 62 (2006) 1002–1011, https://doi.org/10.1107/S0907444906022116.

[59] P. Emsley, K. Cowtan, Coot: model-building tools for molecular graphics, Biol. Crystallogr. 60 (2004) 2126–2132, https://doi.org/10.1107/S0907444904019158.
[60] P.D. Adams, W. Ralf, R.J. Read, J.C. Sacchettini, N.K. Sauter, PHENIX: building new software for automated crystallographic structure determination, Biol. Crystallogr. 58 (2002) 1948–1954, https://doi.org/10.1107/S0907444902016657.
[61] V.B. Chen, B.W. Arendall, J.J. Headd, D.A. Keedy, R.M. Immormino, G.J. Kapral, L. W. Murray, J.S. Richardson, D.C. Richardson, MolProbity: all-atom structure validation for macromolecular crystallography, Biol. Crystallogr. 66 (2010) 12–21, https://doi.org/10.1107/S0907444909042073.